

Uniform Magnetic Order in a Ferromagnetic-Antiferromagnetic Random Alternating Quantum Spin Chain

Tota Nakamura

*Department of Applied Physics, Tohoku University,
Aramaki aza Aoba 05, Aoba, Sendai, Miyagi 980-8579, Japan*

(Dated: May 14, 2019)

An $S = 1/2$ ferromagnetic (F) - antiferromagnetic (AF) random alternating Heisenberg quantum spin chain model is investigated in connection to its realization compound: $(\text{CH}_3)_2\text{CHNH}_3\text{Cu}(\text{Cl}_x\text{Br}_{1-x})_3$. The exchange interaction bonds have alternating strong F-AF random bonds and weak uniform AF bonds. Using the quantum Monte Carlo method we have found that the excitation energy gap closes and the uniform AF order becomes critical in the intermediate concentration region. This finding explains the experimental observation of the magnetic transition by considering weak interchain interactions. Present results suggest that the uniform AF order survives even in the presence of randomly located ferromagnetic bonds. This may be a new quantum effect.

PACS numbers: 75.10.Jm, 75.10.Nr, 75.40.Mg

I. INTRODUCTION

Quantum spin systems have been attracting wide interest both theoretically and experimentally. The quantum effect sometimes produces a conclusion that is quite different from our knowledge of the classical system. Since the effect becomes remarkable in low dimensions, various exotic phenomena have been found in one-dimensional quantum spin systems. The Haldane state in an $S = 1$ antiferromagnetic Heisenberg chain may be the most famous example.¹ These theoretical systems can be realized experimentally. New phenomena predicted theoretically can be observed in experiments, and new findings from experiments can be explained theoretically. The working together of theory and experiment in this field is producing progress in condensed matter physics.

Randomness is another keyword in exotic phenomenon of quantum spin systems. It sometimes brings order to disorder. The appearance of a magnetic order due to impurity doping of a spin-disordered system is a typical example.^{2,3} There is a finite excitation energy gap above the nonmagnetic quantum ground state in the pure concentration compound. Random impurity doping destroys the energy gap, and creates magnetic order. A similar effect can be observed by destroying the energy gap by a uniform magnetic field.

Recently, Manaka et al.⁴ found another example of randomness-induced long-range order phenomena by mixing two spin-gapped compounds with nearly identical structures. One compound is $(\text{CH}_3)_2\text{CHNH}_3\text{CuCl}_3$ (abbreviated as IPACuCl₃), which realizes the $S = 1/2$ ferromagnetic (F)-antiferromagnetic (AF) bond alternation Heisenberg chain with $J_{\text{strong}} \sim 54$ K (F) and $J_{\text{weak}} \sim -23$ K (AF).^{5,6} Because of the strong F bonds, the ground state of this compound is considered to be the Haldane state. The other compound is $(\text{CH}_3)_2\text{CHNH}_3\text{CuBr}_3$ (IPACuBr₃), which realizes the $S = 1/2$ AF-AF bond alternation Heisenberg chain with $J_{\text{strong}} \sim -61$ K (AF) and $J_{\text{weak}} \sim -33$ K (AF).⁷ The

ground state is the singlet dimer state. These two compounds have different origins of the energy gap.

A magnetic phase transition is observed in the intermediate concentration $0.44 < x < 0.87$ of IPACu(Cl_xBr_{1-x})₃ by measurements of the susceptibility and the specific heat. Dependence of the susceptibility on the direction of the external field suggested that the order is antiferromagnetic. The interesting point of this system is that the situation mentioned below is adverse to an existence of any uniform magnetic order. On the other hand, the observed lines of experimental evidence suggest uniform antiferromagnetism. Ferromagnetic bonds are randomly located in the mixed compound. The staggered phase factor of the classical antiferromagnetic order changes its sign randomly depending on the random location of the ferromagnetic bonds. If the interchain interactions are uniformly antiferromagnetic (or ferromagnetic), there also exists randomly located frustration.

In this paper we show that uniform antiferromagnetic order possibly appears in IPACu(Cl_xBr_{1-x})₃. Our results suggest a scenario of the appearance of the order. The scenario can be expanded to explain a general impurity-induced long-range order phenomenon. A theoretical spin model is proposed in Sec. II. We carry out quantum Monte Carlo simulations to this model. The method is explained in Sec. III. The results of the excitation energy gap, the string order parameter, the magnetic susceptibility, and the staggered magnetization are presented in Sec. IV. Section V is devoted to conclusions.

II. MODEL

We consider a theoretical model to explain the experiments on IPACu(Cl_xBr_{1-x})₃. From crystal structure analyses of pure compounds,^{5,6,7} it is known that there are two Cl ions or two Br ions that bridge the magnetic Cu ions: $\text{Cu} \langle \text{Cl} \rangle \text{Cu}$ or $\text{Cu} \langle \text{Br} \rangle \text{Cu}$. The copper ions are linked step-wise along the c -axis. Exchange interactions

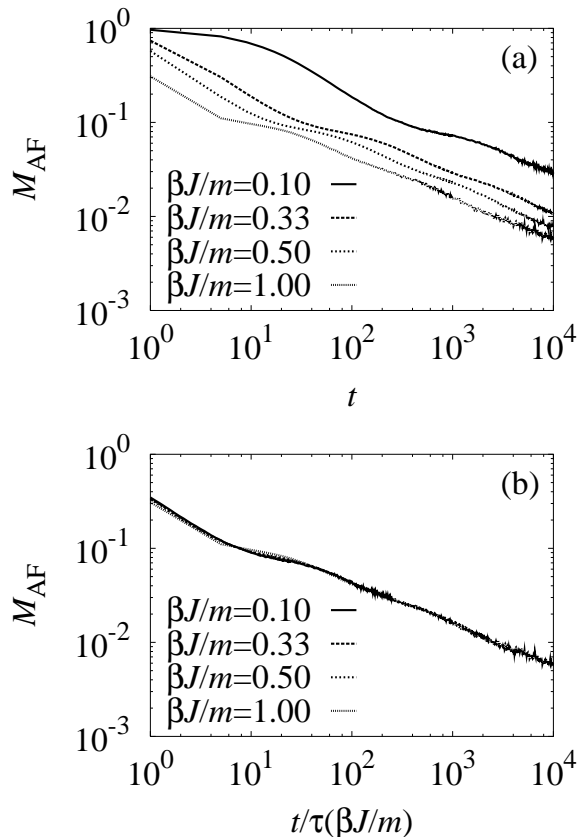


FIG. 2: (a) Relaxation functions of staggered magnetization (M_{AF}) for various choices of Trotter number m . Inverse temperature $\beta J = 50$ for $\beta J/m = 0.10$ and $\beta J = 500$ for the rest. The random bond concentration ratio $p = 0.75$. There is no temperature dependence within 10^4 Monte Carlo steps. Real-space system size is 644 spins for $\beta J/m = 0.10$ and 322 spins for the rest. (b) If the Monte Carlo step is rescaled by $\tau(\beta J/m)$ of each Trotter number, the relaxation functions fall onto the same curve. $\tau(0.10) = 40$, $\tau(0.33) = 4.2$, and $\tau(0.50) = 2.18$.

finite Trotter number²⁴ and verified our argument. It is also checked by comparing NER functions with different Trotter numbers.

Figure 2 shows relaxation functions of staggered magnetization (M_{AF}) when simulation starts from a classical staggered state. The raw relaxation curve is dependent on the Trotter number m as shown in Fig. 2(a). Relaxation becomes slow as the ratio $\beta J/m$ decreases. This is called Wiesler freezing. When the Monte Carlo step is rescaled by a correlation time of each Trotter number, the relaxation curves coincide with each other. Therefore, the behavior of the relaxation function is independent of the Trotter number. We can consider that the data of Fig. 2(b) are the relaxation function in the infinite Trotter number limit. The value of $\beta J/m$ for NER simulations in this paper is fixed at $1/2$ unless otherwise stated.

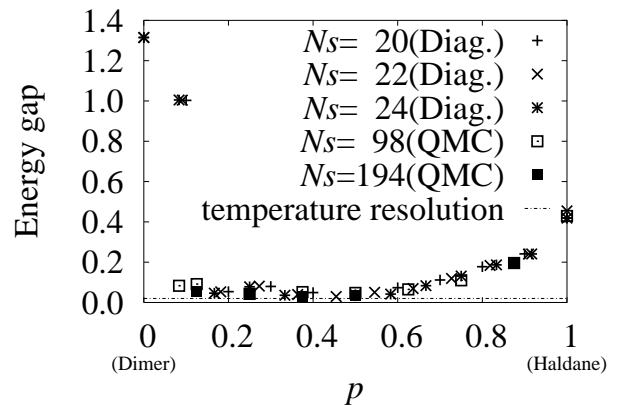


FIG. 3: Excitation energy gap estimated from an energy difference between the subspace with total $S^z = 0$ and that with $S^z = 1$.

IV. RESULTS

A. Excitation energy gap

In this subsection we present results of the excitation energy gap. It is investigated in order to make it clear where the gap closes by an introduction of the random bonds. We adopt two different strategies. One is direct observation of the energy gap. It is calculated from the difference between an energy expectation value in a subspace with total $S^z = 0$ and that in a subspace with total $S^z = 1$. The other is a nonequilibrium relaxation of the local susceptibility χ_{loc} defined by:

$$T\chi_{loc} = \sum_i \left(\frac{1}{m} \sum_{j=1}^m S_{i,j}^z \right)^2 = \frac{2}{\Delta} \sum_i \langle \psi_g | S_i^z | \psi_{ex} \rangle^2. \quad (2)$$

Here, j denotes a location in the Trotter direction in the $(d+1)$ -dimensional lattice. Subscript i denotes a location in the real space direction. Wave functions of the ground state and the first excited state are denoted by ψ_g and ψ_{ex} , respectively. The excitation energy gap is denoted by Δ . Since the local susceptibility is proportional to the inverse of the excitation gap, it diverges in the gapless phase and it converges to a finite value in the gapful phase. The change of behavior identifies the gapless-gapful transition point. We have also performed a finite-time scaling analysis on the relaxation function of $T\chi_{loc}$ and estimated the transition point.

Figure 3 shows the result of direct observation of the energy gap. When the spin number is small ($N_s \leq 24$), we have done numerical diagonalization (Diag.) and estimated the numerically exact value for the energy gap. Here, we have taken averages over all the possible random configurations at each ferromagnetic bond concentration p . When the spin number is large ($N_s \geq 98$), equilibrium quantum Monte Carlo (QMC) simulations are carried out. The temperature is $T/J = 0.01$. Therefore,

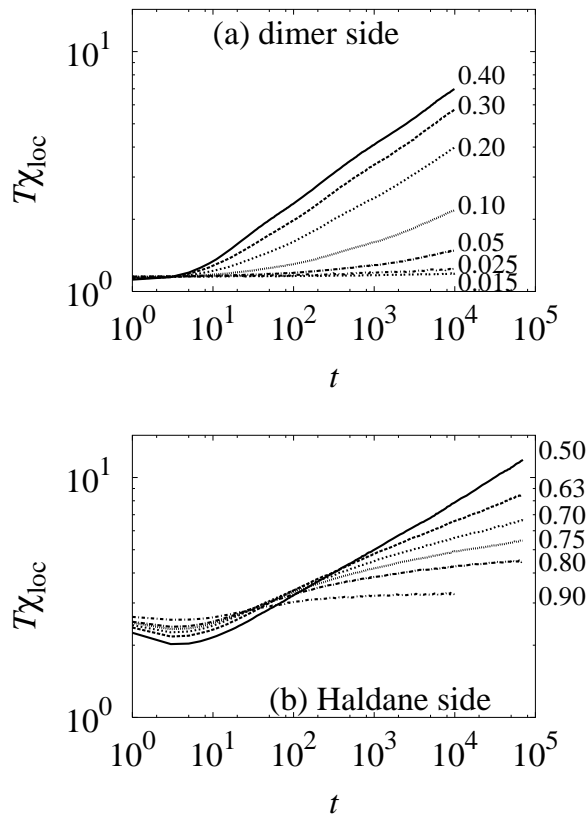


FIG. 4: Nonequilibrium relaxation of the local susceptibility. A value of p is as denoted beside each plot. It exhibits diverging behavior in the gapless phase.

the energy gap resolution is an order of $\sim 0.02J$. Infinite Trotter number extrapolations are performed using ten data between $\beta J/m = 0.38$ and $\beta J/m = 1$. Two thousand random bond configurations are taken.

We call a region $0.5 < p < 1$ a Haldane side hereafter in this paper. At $p = 1$ the Haldane state is realized in the ground state. On the other side $0 < p < 0.5$ the region is called a dimer side. This is because the dimer ground state is realized at $p = 0$. We call $p = 0.5$ a fully-random point.

The energy gap on the Haldane side gradually decreases as random bonds are introduced. It seems that the gap closes at $p \sim 0.6$. On the contrary, the gap on the dimer side suddenly decreases. It suggests that the gap closes by a small randomness. Diagonalization results at $p \sim 0.1$ are strongly affected by finite-size effects.

Figure 4 shows nonequilibrium relaxation plots for the local susceptibility. Simulation starts from a gapful ground state in a pure concentration limit. On the dimer side the dimer ground state is prepared by running a simulation with the pure Hamiltonian at $p = 0$. By changing a random number sequence we have generated a different representation of the ground state for each random bond configuration. On the Haldane side

the Haldane ground state is prepared by a Hamiltonian at $p = 1$ in the same procedure. The spin number is 322, the inverse temperature $\beta J = 500$, and the Trotter number $m = 1000$. For $p = 0.015$ the spin number is 802. The number of random bond configurations is at least two thousand and it is more than ten thousand near the transition point.

Gapless behavior is observed in the region of $0.025 < p < 0.75$. There is a grey zone $0.63 < p \leq 0.75$, where it is hard to identify whether the relaxation function is diverging or converging. Determination of the gapless-gapful transition point on the dimer side is not settled in the present simulations. There is a possibility that a relaxation of $p = 0.015$ starts diverging behavior after $t = 10^4$. It is safe to note that the point is smaller than $p = 0.025$. It is also noted that the exponent of divergence (slope in the figure) is almost independent of p near $p = 0.5$. This suggests that the gapless phase near $p = 0.5$ is characterized by some universal exponent as in the random singlet phase.¹⁵

In order to determine the gapless-gapful transition point on the Haldane side we have performed a finite-time scaling analysis.^{18,20} We plot $T\chi_{\text{loc}}t^{-a}$ versus $t/\tau(p)$ choosing a and $\tau(p)$ properly so that all the relaxation data fall onto the same scaling function. Figure 5 (a) shows the result of scaling. We have used data of eight different p ranging $0.69 \leq p \leq 0.83$. The correlation time $\tau(p)$ is supposed to diverge at the transition point following the KT singularity: $\tau(p) \sim \exp[B/\sqrt{p-p_c}]$. It is shown in Fig. 5 (b). The best fit is achieved by a choice of transition point $p_c = 0.625$. This procedure is a direct interpretation of the finite-size scaling analysis of the KT transition in the $S = 1/2$ alternating ferromagnetic chain introduced by Yoshida and Okamoto.²⁵

Within the accuracy of the present simulations we can only note that the gapful-gapless transition point on the dimer side is located somewhere below $p = 0.025$. Since this value is very small, we may consider that a small randomness immediately destroys the excitation energy gap. Therefore, the gapless phase is considered to exist in the region of $0 < p < 0.625$.

B. String order parameter

The string order parameter is a good order parameter associated with the gapless-gapful transition in a one-dimensional quantum spin system. It reflects a hidden antiferromagnetic symmetry in the gapful phase. On the Haldane side a string order parameter introduced by den Nijs and Rommelse²⁶ is evaluated:

$$O_{\text{str}} = T_i^z \exp \left[i\pi \sum_{k=i+1}^{j-1} T_k^z \right] T_j^z, \quad (3)$$

where we have defined a bond spin $\mathbf{T}_i \equiv \mathbf{S}_{2i} + \mathbf{S}_{2i+1}$. On the dimer side a string order parameter introduced

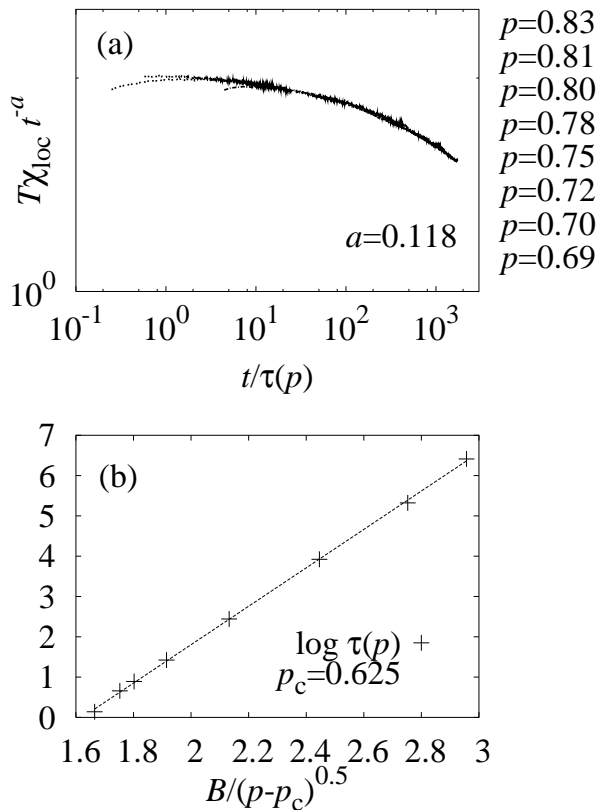


FIG. 5: Finite-time scaling of the local susceptibility on the Haldane side.

by Hida²⁷ is evaluated:

$$O_{\text{dim}} = -4S_{2i}^z \exp \left[i\pi \left(S_{2i+1}^z + \sum_{k=i+1}^{j-1} T_k^z + S_{2j}^z \right) \right] S_{2j+1}^z. \quad (4)$$

These order parameters are considered to take finite values in the gapful phase. It is argued that the string order parameter takes a finite value but the excitation energy gap is zero in the quantum Griffiths phase.^{13,30} Therefore, it is possible to identify this phase comparing the excitation gap results and the string order results.

Figure 6 shows nonequilibrium relaxation functions of the string order parameters. Simulation conditions are the same as those for the local susceptibility. On the Haldane side it exhibits a converging behavior for $p > 0.63$. This is consistent with our estimate for the gapless transition point $p = 0.625$. Therefore, the Haldane phase is considered to exist in a region of $0.625 \leq p \leq 1$. This phase is quite robust against randomness. When the concentration is lowered, the string order parameters decay algebraically, whose exponent is dependent on the concentration. On the dimer side the string order parameters suddenly start decaying by an introduction of random bonds. This is also consistent with the behavior of local susceptibility. The dimer gap state is quite fragile

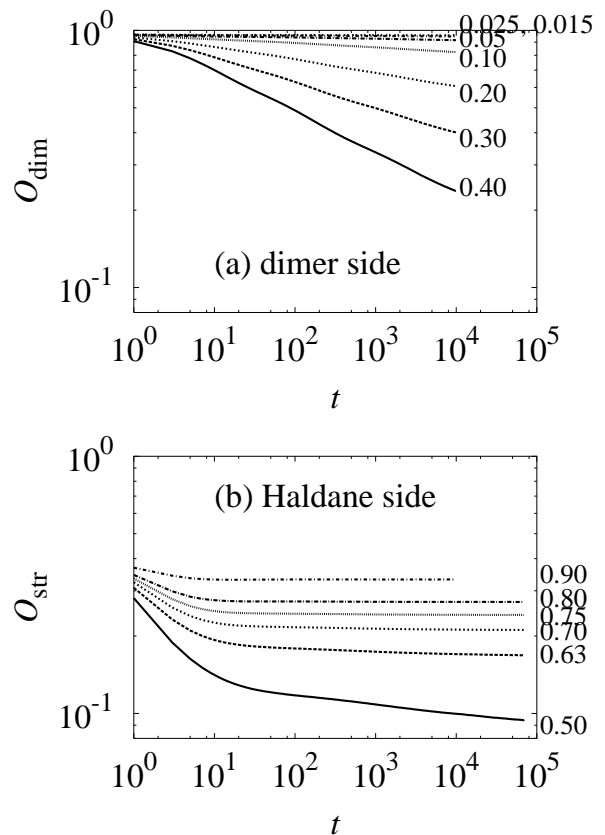


FIG. 6: Nonequilibrium relaxation of the string order parameters. A ferromagnetic bond concentration p is denoted beside the data.

against randomness.

C. The magnetic susceptibility

The ground states in pure concentration limits ($p = 0, 1$) are a spin-disordered state with a finite excitation energy gap. The magnetic susceptibility takes a value of order unity. Starting simulation from this ground state, we observe nonequilibrium relaxation functions of the following two kinds of the magnetic susceptibility. One is the uniform staggered susceptibility. This is intended to check the possibility of criticality of the uniform antiferromagnetic order speculated on by the experiment of $\text{IPACu}(\text{Cl}_x\text{Br}_{1-x})_3$. The other one is the generalized staggered susceptibility, which is the susceptibility associated with the general staggered state. Here, we mean the generalized staggered state in Fig. 7. This is a random classical state which minimizes the S^z part of the Hamiltonian. The susceptibility shows converging behavior if the magnetic order remains disordered. It shows diverging behavior if the magnetic order is critical. In the gapful region estimated in the previous subsections both sets of the susceptibility data should exhibit converging

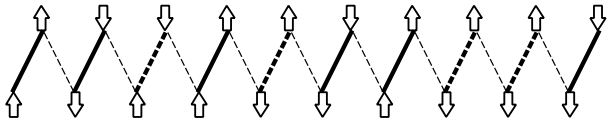


FIG. 7: A generalized staggered state. Arrows depict the S^z representation. Solid lines depict ferromagnetic bonds and broken lines depict antiferromagnetic bonds.

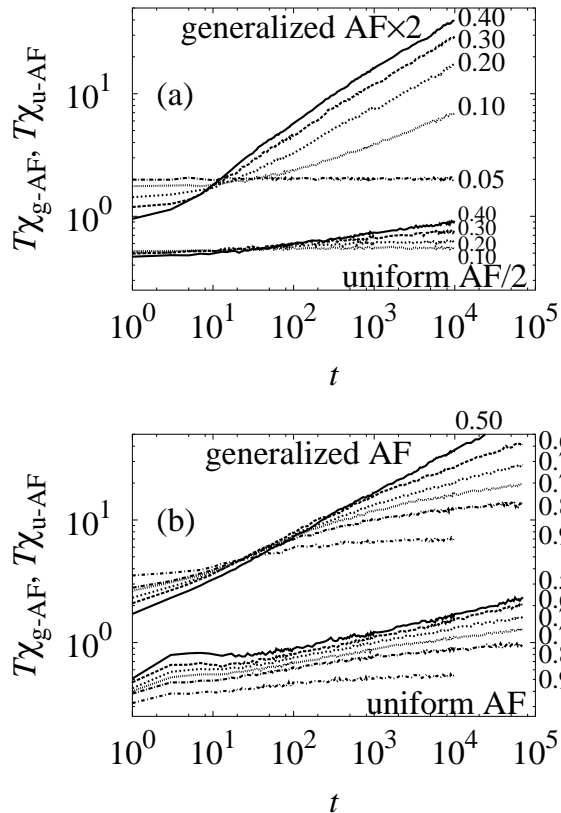


FIG. 8: Nonequilibrium relaxation of the generalized staggered susceptibility χ_{g-AF} and that of the uniform staggered susceptibility χ_{u-AF} . (a) The dimer side. (b) The Haldane side. Both orders exhibit critical behavior in the gapless region $0 < p < 0.625$.

behaviors.

Figure 8 shows nonequilibrium relaxation functions of two kinds of the magnetic susceptibility. Simulation conditions are the same as in the previous subsections. Both sets of the susceptibility data exhibit critical behaviors in the gapless region $0.2 < p < 0.63$. There is a grey zone between $p = 0.63$ and $p = 0.75$ as in the data of the local susceptibility. The raw relaxation data alone cannot show a difference between diverging and converging. At $p = 0.1$ and $p = 0.2$ the generalized staggered susceptibility shows diverging behavior, while the uniform staggered susceptibility remains finite. We discuss this

issue in the next subsection with regard to resolution of the present simulations. In the Haldane phase, relaxation functions also exhibit converging behavior. There is no qualitative difference between the two orders. Amplitude of the uniform staggered susceptibility is smaller than the generalized one. This is because the randomly-located ferromagnetic bonds conflict with the uniform antiferromagnetic order and this decreases the amplitude.

The critical behavior of the uniform antiferromagnetic order in this figure is a new finding in the present random model. It suggests that the order can survive against the randomly located ferromagnetic bonds. This is a purely quantum effect. We cannot expect it in the classical model. In the real compound the uniform antiferromagnetic order can be a long-range order by finite inter-chain antiferromagnetic couplings. In order to check the criticality of this order we observe nonequilibrium relaxation functions of uniform staggered magnetization when we start simulations from the uniform antiferromagnetic state.

D. Uniform staggered magnetization

Uniform staggered magnetization (M_{AF}) is observed to see whether it decays exponentially or algebraically when starting from the uniform antiferromagnetic state. If it exhibits an algebraic decay, this state is proved to be critical as suggested in the previous subsection. The system size of the present simulation is $N = 1601$ (3202 spins), $m = 400$, and $\beta J = 200$. The number of random bond configurations is more than one hundred. The temperature corresponds to ~ 0.1 K which is lower than the experimental ones (the phase transition was observed at 15 K). It is also confirmed that there is no temperature dependence within the time scale the simulations are performed. Therefore, we consider that the ground state is realized. The size of the simulation determines the resolution limit of an obtained physical quantity. The resolution of the staggered magnetization is of the order of $1/\sqrt{2mN} \times (\text{number of samples}) \leq 10^{-4}$. On the other hand, the resolution of the susceptibility in the previous subsection is of the order of J/T , which corresponds to the AF magnetization per spin $\langle M_{AF} \rangle \sim 1/\sqrt{mN} \sim 3 \times 10^{-3}$. Both simulations are consistent when within the resolution of $\langle M_{AF} \rangle > 10^{-3}$.

Figure 9 shows nonequilibrium relaxation of staggered magnetization. We have also plotted the result of the $S = 1/2$ uniform antiferromagnetic Heisenberg chain, which is exactly solved and the AF order is critical. In the intermediate region, the relaxation function exhibits algebraic decay after an initial relaxation that rides on relaxation of the pure gapful system. Note that the length of the initial relaxation, $t < 50$, agrees with that of the susceptibility simulations in Fig. 8. The relaxation functions of the susceptibility begin diverging behaviors after 50 Monte Carlo steps.

The numerical value of the staggered magnetization

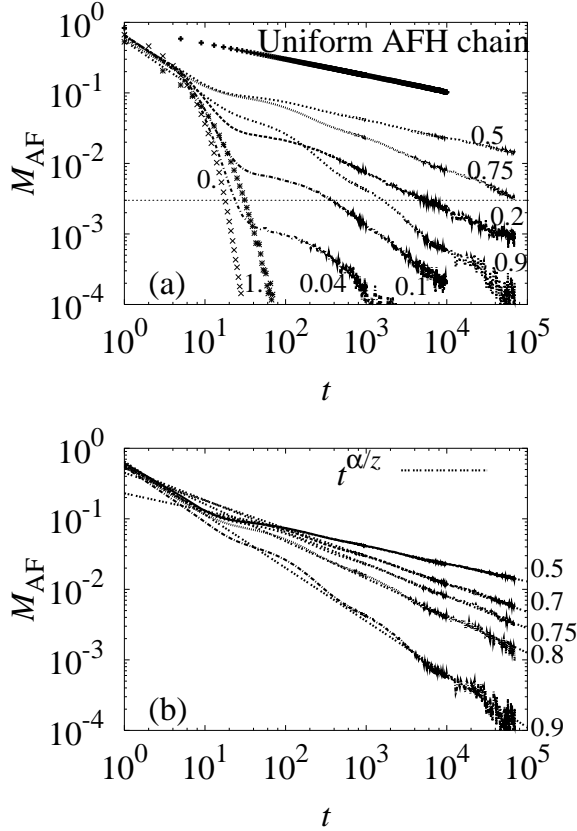


FIG. 9: (a) Nonequilibrium relaxation of uniform staggered magnetization when simulation starts from the uniform AF state. The value of the ferromagnetic bond concentration p is denoted beside each plot. Relaxation functions of the pure concentration limit, $p = 0$ and $p = 1$, and that of the $S = 1/2$ uniform antiferromagnetic Heisenberg (AFH) chain are also plotted by symbols. (b) Relaxation functions on the Haldane side can be fitted by $t^{\alpha/z}$, which is analytically obtained by a real-space renormalization procedure.

at which the relaxation begins to exhibit critical behavior is roughly considered as the magnitude of the order. At $p = 0.1$, an algebraic decay begins below the susceptibility resolution limit 3×10^{-3} . Therefore, algebraic divergence cannot be observed at $p = 0.1$ in Fig. 8. It is difficult to estimate the resolution of the experiment observing the magnetic phase transition. However, if one assumes it to be $\langle M_{AF} \rangle \sim 10^{-3}$, the numerical results presented in this paper quantitatively explain the experimental results. The experiment can detect the phase transition at $p = 0.2$ because the amplitude of the magnetic order is $\langle M_{AF} \rangle \sim 10^{-2}$, where the algebraic decay begins in Fig. 9(a). This bond concentration corresponds to the Cl atom concentration $x = 0.45$ by $p = x^2$. This value coincides with the experimental limit of observing the phase transition: $x = 0.44$. At $p = 0.1$ the amplitude of the magnetic order is about 10^{-3} . It is difficult for the experiment to detect this small magnetic order.



FIG. 10: Depletion procedure of a strong antiferromagnetic bond on the Haldane side.

Within the accuracy of Fig. 9(a), the phase boundary on the dimer side resides between $p = 0.04$ and $p = 0.1$. This corresponds to between $x = 0.2$ and $x = 0.3$, which is lower than the experimental observation. When the resolution of the experimental probe becomes sharper, the magnetic phase may be observed in a wider region. The same argument is possible in our simulations. If resolution of our simulation becomes sharper, the critical behavior can be observed in a wider region. A true phase boundary may be located at a concentration lower than $p = 0.04$. The present estimate is the upper limit due to the limited numerical resolution.

For $p > 0.75$, the relaxation shows multi-exponential decay, suggesting a discrete distribution of the energy gap. As p decreases, the relaxation appears to be an algebraic decay. At the fully random point $p = 0.5$, the magnetization takes a maximum value. The slope at this point is almost the same as that of the $S = 1/2$ uniform AFH spin chain with the amplitude reduced to $1/4$. This is a notable finding in this paper. The fully random chain exhibits the antiferromagnetic criticality which is qualitatively equivalent to the nonrandom uniform AFH chain. This behavior guarantees again the observation of a weak antiferromagnetic phase transition assisted by weak interchain interactions in the real compound.

Algebraic decay in the intermediate region can be explained by the power-law distribution of the energy gap. On the Haldane side ($p > 0.5$), we can consider the strong antiferromagnetic bonds as impurities that can be replaced by effective weak bonds. A singlet dimer state can be easily formed on an isolated strong antiferromagnetic bond. Then, spin degrees of freedom on this bond freeze. We may deplete this singlet spin pair and connect the neighboring spins by a new effective interaction bond. This procedure is depicted in Fig. 10. A new effective bond is estimated to be $((-J)^2/2 * -2J) = -J/4$ by the second-order perturbation theory. As long as successive perturbation is good, the strength of the effective bond replacing n aligned strong antiferromagnetic bonds is $\exp[-\lambda n]J$ with $\lambda = \log 4$. The probability of the occurrence of this configuration is $(1-p)^n$. Then, the distribution of the effective bonds is^{8,10}

$$P(J) \sim \frac{1}{\lambda} J^{-1 + \frac{1}{\lambda} \log \frac{1}{1-p}} \propto \alpha J^{-1+\alpha}, \quad (5)$$

with $\alpha = (1/\lambda) \log(1/(1-p))$. Because the Valence-Bond-Solid picture is valid in this region, the singlet dimers are located on the weak antiferromagnetic bonds between the strong ferromagnetic bonds. This bond distribution is directly interpreted by the gap distribution

$P(\Delta)$. This distribution is equivalent to that in the random singlet phase, $P(\Delta) = \alpha\Omega^{-\alpha}\Delta^{\alpha-1}$, with a characteristic energy scale Ω .¹⁵ Each energy gap contributes to the exponential decay of the staggered magnetization with a contribution $\exp[-\Delta^z t]$ (z : the dynamic exponent). The sum of these exponential decays by the distribution $P(\Delta)$ becomes an algebraic decay as

$$\int \exp[-\Delta^z t] P(\Delta) d\Delta = \Gamma(\alpha/z + 1)(t/\tau)^{-\alpha/z}, \quad (6)$$

with a characteristic time scale $\tau \sim \Omega^{-z}$. Therefore, the staggered magnetization is expected to decay algebraically with the exponent $\alpha/z = (1/z\lambda) \log(1/(1-p))$, which is dependent on the concentration p . The slope of the algebraic decay in Fig. 9 (b) quantitatively agrees with this expression supposing $z = 2.2$ for $p > 0.6$ and $z = 2.0$ for $0.5 \leq p < 0.6$. The value $z = 2.2$ is consistent with the two-dimensional classical Ising model. The value $z = 2.0$ means that the dynamics of the Monte Carlo simulation are governed by pure diffusion. It suggests a random singlet phase.

On the dimer side ($p < 0.5$), interpretation is not straightforward. It is not good to deplete the strong antiferromagnetic bonds which are the majority. Depletion of the strong ferromagnetic bonds (the Haldane cluster) is possible, and weak effective bonds of the amplitude $\exp[-\lambda'n]$ ²⁸ may replace them. We can obtain the same critical behavior by this procedure. However, the estimated values of the exponent α/z do not coincide with the numerical results.

E. Phase diagram

Putting all the results together we draw a phase diagram of the present model in Fig. 11. The corresponding experimental results are also drawn. The excitation energy gap and the string order parameter remain finite in the region $0.75 \leq p \leq 1$. This phase boundary $p = 0.75$ is a special point. It is pointed out by Hida²⁹ that the Haldane phase is stable as long as the gap distribution is not singular at $\Delta = 0$. It corresponds to $p = 0.75$ ($x = 0.87$) by $\alpha = 1$ in the present model. The relaxation functions of Fig. 9 exhibit multi-exponential decay for $p > 0.75$. Therefore, this region is considered the Haldane phase. The phase boundary of the experimental results is also located at $p = 0.75$. It is very likely that the experiments^{4,12} detected this quantum phase transition point.

There is a grey zone between $p = 0.625$ and $p = 0.75$. A string order parameter seems to remain finite. Raw relaxation functions of the local susceptibility suggest that the excitation gap is zero. However, scaling analysis suggests that the gap is finite. Except for the scaling result these lines of evidence suggest this region is the quantum Griffiths (QG) phase: no excitation gap and a finite string order. However, classical magnetic orders exhibit

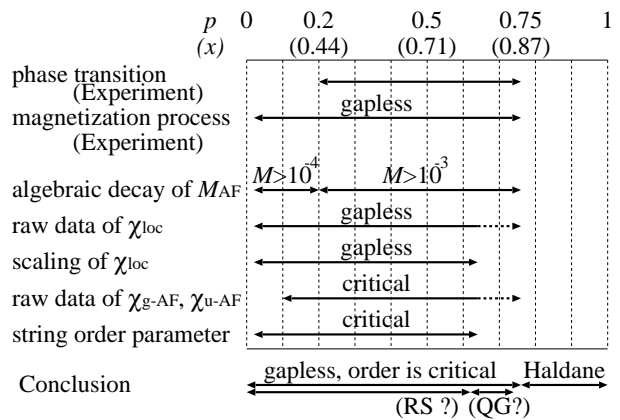


FIG. 11: A phase diagram concluded in this paper.

critical behavior in this region. It is not settled whether this phase is the QG phase or not.

It was also reported by Yang and Hyman³⁰ that the random singlet phase begins at $\alpha \sim 0.67$ for the algebraic bond distribution $P(J) \sim \alpha J^{-1+\alpha}$. This point corresponds to $p \sim 0.6$. In the neighborhood of the fully random point, $0.4 < p < 0.6$, an exponent of the local susceptibility is weakly dependent on p , suggesting a universal phase. At the fully random point $p = 0.5$, however, relaxation of the uniform staggered magnetization is qualitatively the same as the uniform $S = 1/2$ antiferromagnetic Heisenberg chain. The classical magnetic order is critical in this phase. It is not clear whether this evidence is compatible with the random singlet (RS) phase or not. Therefore, we put a question mark for the RS phase and QG phase in our phase diagram Fig. 11.

V. CONCLUSIONS

In this paper the magnetic ordered phase observed in the experiment of IPACu(Cl_xBr_{1-x})₃ is explained. The magnetic structure is made clear to be the uniform antiferromagnetic order. The phase boundaries estimated in the simulation quantitatively agree with the experimental results.

Behaviors of the relaxation functions in Fig. 9(a) suggest the following scenario for the appearance of magnetic order. Short-range antiferromagnetic correlations are first destroyed by local singlet dimer states or local Haldane states that appear during the initial relaxation of exponential decay ($t < 100$). Beyond these local states, there exist very weak but finite effective interactions. This is because local singlet states or local Haldane states are not the exact eigenstate of the total Hamiltonian. The effective interactions obey the power-law distribution as in Eq. (5). They are considered to produce local excitation gaps. Then, the magnetic order decays exponentially by this excitation gap. The sum of the exponential decays due to these effective interactions

becomes the algebraic decay as seen in Eq. (6). This is considered to be the origin of the criticality of the uniform antiferromagnetic order. Magnetic order is observed in the experiment with the help of the interchain interactions. The present phenomenon is quite interesting because the uniform antiferromagnetic order survives despite the randomly located ferromagnetic bonds. This may be a new exotic quantum phenomenon. The role of the ferromagnetic bonds in the quantum system should be reconsidered.

It is also noted that the present mechanism explains the general impurity-induced long-range order phenomenon.^{2,3} Randomly doped impurities divide a spin chain into local gapful clusters linked together with small but finite interactions. The edge spins of the cluster correlate with each other by effective bonds which exhibit

the power-law distribution. Collections of the correlation become the algebraic decay as in Eq. (6). Therefore, any classical ordered state can be critical. In the real compounds, an order whose amplitude is the largest and/or an order which does not conflict with the interchain interactions will be selected.

Acknowledgments

The author would like to thank Dr. H. Manaka and Professor K. Hida for their fruitful discussions and comments. Use of the random number generator RNDTIK programmed by Professor N. Ito and Professor Y. Kanada is gratefully acknowledged.

-
- ¹ F. D. M. Haldane, Phys. Rev. Lett. **50**, 1153 (1983).
² M. Hase et al., Phys. Rev. Lett. **71**, 4059 (1993).
³ M. Azuma et al., Phys. Rev. B **55**, R8658 (1997).
⁴ H. Manaka, I. Yamada and H. Aruga Katori, Phys. Rev. B **63**, 104408 (2001).
⁵ H. Manaka, I. Yamada and K. Yamaguchi, J. Phys. Soc. Jpn. **66**, 564 (1997).
⁶ H. Manaka, I. Yamada, Z. Honda, H. Aruga Katori and K. Katsumata, J. Phys. Soc. Jpn. **67**, 3913 (1998).
⁷ H. Manaka and I. Yamada, J. Phys. Soc. Jpn. **66**, 1908 (1997).
⁸ K. Hida, Prog. Theor. Phys. Suppl. **145**, 320 (2002).
⁹ T. Nakamura, Prog. Theor. Phys. Suppl. **145**, 353 (2002).
¹⁰ K. Hida, J. Phys. Soc. Jpn. **72**, 688 (2003).
¹¹ T. Nakamura, J. Phys. Soc. Jpn. **72**, 789 (2003).
¹² H. Manaka, I. Yamada, H. Mitamura and T. Goto, Phys. Rev. B **66**, 064402 (2002).
¹³ R. A. Hyman and K. Yang, Phys. Rev. Lett. **78**, 1783 (1997).
¹⁴ S. K. Ma, C. Dasgupta and C. -K. Hu, Phys. Rev. Lett. **43**, 1434 (1979).
¹⁵ D. S. Fisher, Phys. Rev. B **50**, 3799 (1994).
¹⁶ N. Ito, Physica A **196**, 591 (1993).
¹⁷ N. Ito and Y. Ozeki, Intern. J. Mod. Phys. **10**, 1495 (1999).
¹⁸ Y. Ozeki, K. Ogawa and N. Ito, Phys. Rev. E **67**, 026702 (2003).
¹⁹ Y. Nonomura, J. Phys. Soc. Jpn. **67**, 5 (1998).
²⁰ T. Shirahata and T. Nakamura, Phys. Rev. B **65**, 024402 (2002).
²¹ T. Nakamura and S. Endoh, J. Phys. Soc. Jpn. **71**, 2113 (2002).
²² T. Nakamura, S. Endoh and T. Yamamoto, J. Phys. A: Math. Gen. **36**, 10895 (2003).
²³ T. Shirahata and T. Nakamura, J. Phys. Soc. Jpn. **73**, 254 (2004).
²⁴ T. Nakamura and Y. Ito, J. Phys. Soc. Jpn. **72**, 2405 (2003).
²⁵ S. Yoshida and K. Okamoto, J. Phys. Soc. Jpn. **58**, 4367 (1989).
²⁶ M. den Nijs and K. Rommelse, Phys. Rev. B **40**, 4709 (1989).
²⁷ K. Hida, Phys. Rev. B **45**, 2207 (1992).
²⁸ M. Hagiwara et al., Phys. Rev. Lett. **65**, 3181 (1990).
²⁹ K. Hida, Phys. Rev. Lett. **83**, 3297 (1999).
³⁰ K. Yang and R. A. Hyman, Phys. Rev. Lett. **84**, 2044 (2000).